



**Environmental
Science**
Water Research & Technology

**Modeling the Hydrological Benefits of Green Roof Systems:
Applications and Future Needs**

Journal:	<i>Environmental Science: Water Research & Technology</i>
Manuscript ID	EW-CRV-03-2023-000149.R1
Article Type:	Critical Review

SCHOLARONE™
Manuscripts

Water Impact Statement

A range of modelling approaches have been developed to assess green roof performance to manage stormwater. The appropriateness and efficacy of a given model depend on its capabilities and complexity. This comprehensive review of existing tools, including parameterization, evaluation, and identification of key research gaps can facilitate model improvements to critically evaluate green roof implementation for stormwater management.

Modeling the Hydrological Benefits of Green Roof Systems: Applications and Future Needs

Zhaokai Dong,^a Daniel J Bain,^b Kimberly A Gray,^c Murat Akcakaya^d and Carla Ng^{*a}

^a Department of Civil and Environmental Engineering, University of Pittsburgh, Pittsburgh, PA 15261 USA.

^b Department of Geology and Environmental Science, University of Pittsburgh, Pittsburgh, PA 15261 USA.

^c Department of Civil and Environmental Engineering, Northwestern University, Evanston, IL 60208 USA.

^d Department of Electrical and Computer Engineering, University of Pittsburgh, Pittsburgh, PA 15261 USA.

* Corresponding author email: carla.ng@pitt.edu

Abstract

Green roof (GR) systems provide a promising stormwater management strategy in highly urbanized areas when limited open space is available. Hydrological modeling can predict the ability of GR to reduce runoff. This paper reviews three popular types of GR models with varying complexities, including water balance models, the U.S. EPA's Stormwater Management Model (SWMM), and Hydrus-1D. Developments and practical application of these models are discussed, by detailing model parameter estimates, performance evaluations and application scopes. These three models are capable of replicating GR outflows. Water-balance models have the smallest number of parameters (≤ 7) to estimate. Hydrus-1D requires substantial parameterization effort for soil hydraulic properties but can simulate unsaturated soil water flow processes. Although SWMM has a large number of parameters (>10), it can simulate water transport through the entire GR profile. In addition, SWMM GR models can be easily incorporated into SWMM's stormwater model framework, so it is widely used to simulate the watershed-scale effects of GR implementations. Four research gaps limiting GR model applications are identified and discussed: drainage mat flow simulations, soil characterization, evapotranspiration estimates, and scale effects of GR. The literature document promising results in GR simulations for rainfall events, however, a critical need remains for long-term monitoring and modeling of full-scale GR systems to allow interpretation of both internal (substrate) and external (meteorological characteristics) system effects on stormwater management.

Key words: green roof, hydrological modeling, stormwater management, green infrastructure

1 Introduction

Urban flooding and water pollution are common in cities. Urbanization increases impervious surfaces, increasing velocity/volume of stormwater runoff and downstream pollutant loads to waterbodies.¹⁻³ To mitigate potential environmental impacts of stormwater, alternative approaches for stormwater management have been developed. These approaches shifted from traditional practices (sewer systems) to source control methods that detain, store and treat stormwater on-site.⁴ Green infrastructure (GI) aims to restore, mimic and maintain natural hydrological conditions by using decentralized nature-based practices⁵ and has emerged as one

42 of the most promising and popular stormwater management strategies⁶⁻⁸.

43 Green roofs (GR) are vegetated rooftops, a GI approach that can provide green space in
44 developed areas with limited space for ground-level implementation of GI. In addition, their
45 benefits such as esthetics and thermal performance make them popular in highly urbanized
46 areas.^{9,10} For example, in 2019, there were 763 projects across North America (approximately
47 289190 m² green roofing).¹¹ Based on estimates, the areas of installed GRs can retain 0.14
48 million m³ of stormwater per year. Although the GR industry is estimated to have grown by 5-
49 15% since 2013, there is still an enormous potential roof area of billions of m² for new GRs to
50 be installed at a more rapid rate.

51 GR often consist of a multi-layered construction: a waterproof membrane, a drainage layer, a
52 filter fabric and a substrate layer (soil and plants), built sequentially upward on the roof deck.¹²
53 Based on the substrate depth, GRs are usually categorized as intensive or extensive: intensive
54 GRs have a soil depth larger than 15 cm while extensive GRs have a medium depth less than
55 15 cm.¹³ Extensive GRs are cheaper and require less maintenance¹⁴, but they may be less
56 efficient, compared to intensive GR in stormwater retention and flow rate attenuation¹⁵.
57 However, considering the applicability of retrofitting existing rooftops without adding large
58 loads and additional strengthening, the extensive GRs are more widely used.¹⁶⁻¹⁹

59 Numerous studies have reported GR can reduce stormwater runoff up to 90% and peak flow
60 rates up to 80% during rainfall events.²⁰⁻²⁵ However, the effectiveness of GR to reduce
61 stormwater runoff varies across sites and depends largely on physical properties (substrate
62 depth, roof slopes and vegetation cover)^{21,26,27} and local climate characteristics²⁸. To promote
63 and guide GR implementation, many models of GR hydrological behavior have been created
64 to evaluate GR intrinsic structural properties and the role of external meteorological forcing.²⁸⁻³⁰

65 GR simulations can be classified in two categories: individual scale simulations and
66 watershed/citywide scale simulations. A large portion of the research focuses on developing
67 models to predict GR on-site hydrological processes. These models varied from simple
68 conceptual models^{25,31-33} to complex mechanistic models³⁴⁻³⁷. Their ultimate goals are to
69 develop robust models that can evaluate water transport within GR with varied designs under a
70 range of climatic conditions. However, although studies achieved promising modeling results
71 that replicated GR outflow, uncertainties in model performance remain. For example,
72 Broekhuizen et al. compared the performance of four different models of Urbis, SWMM,
73 Hydrus-1D and Mike SHE to predict GR outflow in Lyon, France and Umeå, Sweden.³⁷ They
74 found inconsistent predictions of flow rates among models suggesting the four models suffer
75 from inadequacies in representations of GR physical processes. In addition, large-scale
76 simulations are vital tools for better understanding the effects of GR implementation in urban
77 stormwater management. Several studies simulated the effects of different GR retrofitting
78 scenarios on runoff/pipe flow reduction.³⁸⁻⁴⁰ Yet, compared to building scale simulations,
79 research on watershed scale simulations is still less common, because the reliability of GR
80 models is often questioned as a design tool.⁴¹ As a result, efforts are needed to identify model
81 limitations and improve model applicability.

82 Li and Babcock (2014) conducted an early review that briefly compared 15 case studies of GR
83 modeling, including SWMM and Hydrus-1D, among others.⁴² However, given limited
84 modeling applications prior to 2010, this review did not cover the modeling techniques that
85 have become available in recent years. While four more recent reviews have discussed GI

86 modeling applications and future needs, they focused on various other types of GI technologies
87 rather than GRs.^{43–46} Different types of GI may require different modeling strategies due to their
88 varied structural designs. For example, a storage zone for exfiltration is commonly used in
89 bioretention systems but is rare in GR systems⁴⁵. None of the previous modeling reviews
90 focused specifically on parameter estimates, evaluation, applications, and gaps in GR modeling.
91 A comprehensive review covering model theoretical developments through practical uses, thus,
92 could provide valuable insights to address the challenges in current applications and future
93 improvements.

94 Focusing on GR modeling techniques and strategies, literature was reviewed to document
95 currently available knowledge, potential challenges and future research needs in GR modeling.
96 More specifically, this review focused on evaluating widely used free and open-source models
97 or software, including water balance models, SWMM, and Hydrus-1D. The review addressed
98 two specific areas: 1) GR model developments and potential applications; 2) identifying and
99 discussing the key limitations in current GR modeling practices with suggestions for future
100 model improvements.

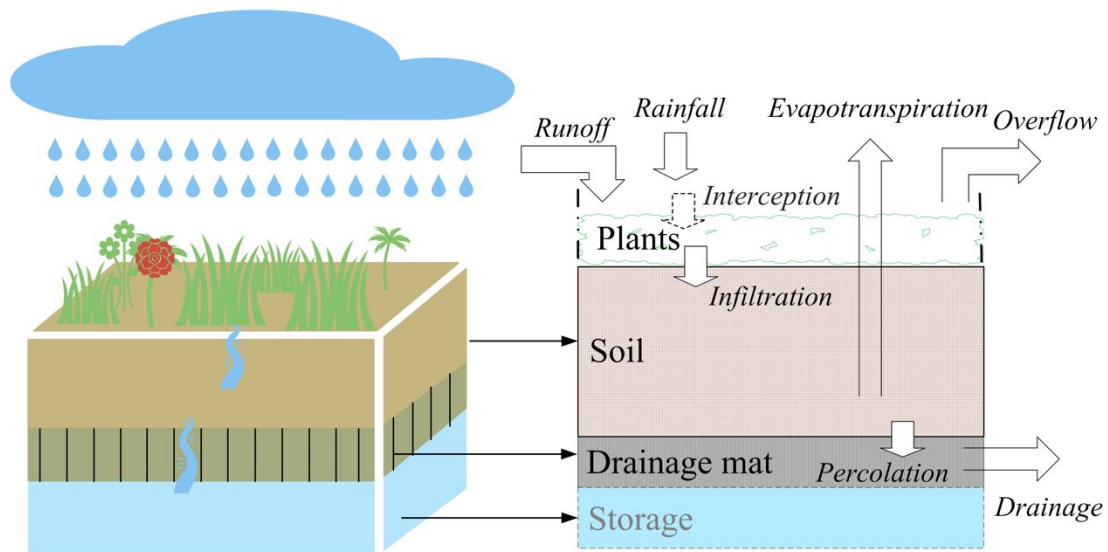
101 2 Methods

102 This review was carried out in the database of Web of Science and ScienceDirect focusing on
103 peer-reviewed primary literature (up to 2022) that aimed to model the hydrological performance
104 of GR. Models built based on full-scale installations as well as pilot-scale experiments were
105 included. To efficiently connect pieces of information most relevant to GR hydrological
106 modeling, the literature search was based on the following keywords: “green roof AND (model
107 or simulation) AND (water balance or hydrology or water or retention) NOT (heat or energy)”.
108 The initial exclusion criteria include review papers, non-English publications and duplicates.
109 We then screened the results based on their abstracts and main content to exclude data analyses,
110 field monitoring, or design papers that are irrelevant to modeling. Meanwhile, additional
111 articles were identified by reviewing the cited references of reviewed papers for articles related
112 to hydrological modeling. Ultimately, 76 peer-reviewed papers were considered as relevant
113 studies and included in the literature review. The review is organized into four sections (Section
114 3 – Section 6). The Section 3 gives an overview of existing GR models and their theoretical
115 developments. In the Section 4, we discuss GR models in practical uses. In the Section 5, we
116 identify potential limitations and challenges for GR model applications. The Section 6 discusses
117 future research needs to improve model applicability.

118 3 Green roof model development

119 3.1 Overview of GR models

120 To physically characterize a GR, it is often simplified as a vertically layered structure with
121 uniform properties within each component (Fig. 1), in which vegetation, soil (substrate),
122 drainage mat and storage can be described separately. GR modeling requires the
123 characterization of the water cycle within these components. The main hydrological processes
124 include rainfall entering soil through infiltration, soil water percolating into drainage mat and
125 water leaving GR by drainage (outflow), evapotranspiration and surface overflow that might
126 occur. Hence, the main research question for GR simulation becomes how to reasonably
127 establish a model incorporating estimates of water budget terms and physical representations
128 of GR structure.



129

130 **Fig. 1** Components and water fluxes of a simplified GR model. Four layers from top to
 131 bottom: vegetation, soil, drainage mat and potential storage units, such as a cistern³², for water
 132 storage and reuse purposes

133 Existing GR models varied from simple conceptual models to complex mechanistic models,
 134 depending on model complexity and the level of detail required to run simulations.^{14,47} A
 135 conceptual model keeps the physical basis of GR but requires little structural detail, such as a
 136 water balance model. Mechanistic models use finite difference equations to model soil water
 137 movement. These models often relate to solving Richard's equations (partial differential
 138 equations to describe water moving through unsaturated soil) or simplified infiltration
 139 equations (often assume saturation). For example, two free software packages, SWMS_2D and
 140 hydrus-1D⁴⁸⁻⁵⁰, apply Richard's equations to numerically derive soil water movement under
 141 unsaturated conditions, with model parameters based on specific soil textures^{51,52}. Solving
 142 Richard's equations usually requires a high level of computational cost. As an alternative,
 143 simplified physically based infiltration equations are utilized by modelers. For example, She
 144 and Pang (2010) used the Green-Ampt infiltration method to simulate GR and successfully
 145 replicated the outflow from a GR in Portland, Oregon.⁵³ This method was also used in the
 146 popular industry standard US EPA's Storm Water Management Model (SWMM) to simulate
 147 infiltration.⁵⁴

148 The sections below discuss the theoretical developments of popular GR models and simulations
 149 of major hydrological processes within GR. The discussions focus on GR models with physical
 150 basis that can be easily interpreted. Therefore, empirical models are not included, because they
 151 are built based on empirical rainfall-runoff relationships and may not be directly applicable in
 152 GR forecasting contexts, for example the Curve Number method^{25,31,37,55}. In addition, in recent
 153 years, data-driven methods such as machine learning techniques have been investigated⁵⁶. Yet,
 154 data-driven methods will not be discussed either, because field data scarcity is a common issue
 155 that managers and developers face to train and test models. Other software packages, such as
 156 MUSICX⁵⁷, have previously been considered for green roof modeling, but as these are not as
 157 widely used and either require licenses for use or are not open source, they will not be discussed.
 158 A summary of all the reviewed GR models can be found in **Error! Reference source not found.**
 159 and **Error! Reference source not found.** (Supporting Information, SI).

160 Three models were selected to be discussed in detail: water-balance models, SWMM and
 161 Hydrus-1D. The complexity of the three models varied from describing conceptual
 162 hydrological processes to solving complex partial differential equations. These models focus
 163 on one-dimensional vertical flow simulations. Because GR substrate is thin compared to roof
 164 surface flow length, water travels more quickly through the substrate vertically than laterally
 165 across it.⁵⁸ Descriptions of the models' capabilities to simulate hydrological processes within
 166 GR are discussed below.

167 3.2 Modeling soil water transport

168 Stormwater control mostly relates to the mechanical process of water movement (infiltration)
 169 within GR substrate.^{30,56,59} Simulation of soil water transport, thus, is the key to building GR
 170 models. In the next subsections, we discuss the simulations of soil water transport processes in
 171 different models.

172 3.2.1 Water balance model

173 A water balance model uses simplified descriptions of water fluxes based on water balance to
 174 account for all sources and fluxes of water through the GR^{19,29}. Simulations can vary from
 175 minutes to daily timesteps^{19,32}. The processes can be described by a finite difference (eq. 1).

$$176 \frac{ds}{dt} = P + I - ET - q - q_s - L \quad \text{eq. 1}$$

177 Where the $\frac{ds}{dt}$ represents the water storage (s) per unit time (t), P is precipitation, I is irrigation,
 178 ET is evapotranspiration, q is drainage (outflow), q_s is surface runoff, L is vegetation
 179 interception; the irrigation and surface runoff terms are often assumed to be negligible.

180 Soil water flow is generated when soil water exceeds the maximum water storage capacity in
 181 the GR substrate.⁶⁰⁻⁶² This capacity can be estimated as the soil depth multiplied by the
 182 difference between the soil field capacity and the permanent wilting point.^{19,60,63} The flow
 183 condition can also be written in the format of soil moisture content exceeding the field
 184 capacity.^{29,61} Therefore, the outflow from beneath of the substrate can be directly derived based
 185 on measured or estimated water budgets of P , ET and s , described as eq. 2, where P_t is rainfall
 186 rate at the current time step t , s_{fc} is the soil water storage capacity and s_{t-1} is water storage at
 187 the previous time step.

$$188 q = \begin{cases} P_t + s_{t-1} - s_{fc} - ET_{t-1}, & s_{t-1} > s_{fc} \\ 0, & s_{t-1} < s_{fc} \end{cases} \quad \text{eq. 2}$$

189 However, this method ignores the dynamics of soil water transport (hydraulic conductivity)
 190 related to water potentials. That is, all the water will drain away within one time step if no
 191 governing equations on moisture transport was introduced, when $s_{t-1} > s_{fc}$. Therefore, to
 192 enable predictions of water storage in the substrate, modelers utilize linear or non-linear
 193 (exponential) lumped reservoirs to describe q based on s , by incorporating two parameters that
 194 approximately represent the ease of water movement^{32,63-66}. The process can be described by
 195 eq. 3, where k_1 , k_2 , φ_1 and φ_2 are fitting parameters, and h is the surface ponding head. A linear
 196 reservoir model corresponds to φ and k equal 1.

$$197 \quad q = \begin{cases} k_1 \cdot (s_{t-1} - s_{fc})^{\varphi_1} + k_2 \cdot h^{\varphi_2}, & s_{t-1} > s_{fc} \\ 0, & s_{t-1} < s_{fc} \end{cases} \text{ eq. 3}$$

198 3.2.2 SWMM

199 SWMM is a dynamic rainfall-runoff model primarily used for urban water quantity and quality
 200 simulations. It allows simulation of interactions among precipitation, urban sewer systems, land
 201 surface, groundwater and GI.⁶⁷ Simulations of GR in SWMM have been developed in several
 202 phases. Before the low impact design (LID) modules were released, GR simulations were built
 203 solely based on SWMM hydrological and hydraulic packages. Alfredo, Montalto, and
 204 Goldstein (2010) developed two strategies based on storage node and the Curve Number
 205 method, respectively, to simulate the GR runoff.⁶⁸ Even though the two approaches could
 206 replicate actual roof discharges, their performance mainly depended on model calibration and
 207 lacked structural representation of GR. With demands for generalizable GI simulations, the LID
 208 modules were released in SWMM 5.0.19 (2010), including modules of bioretention cells,
 209 pervious pavers and infiltration trenches. These modules were built based on process-based
 210 continuous equations to describe water transport within each GR layer (Fig. 1.⁵⁴ The GR module
 211 was added to SWMM 5.1, in which the storage layer was replaced by a drainage mat to simulate
 212 GR underdrains. Because SWMM can easily combine GR models into its stormwater model
 213 framework, it has become a powerful and popular tool to understand city-level hydrological
 214 benefits of GR.^{36,40,50,69-71}

215 GR simulations can be achieved by SWMM GR module or SWMM bioretention module. The
 216 infiltration (f , eq. 4) is modeled using Green-Ampt equation⁷² in the two modules.

$$217 \quad f = K_s \left(1 + \frac{(\phi - \theta_i)(d + \psi)}{F} \right) \text{ eq. 4}$$

218 Where K_s is the saturated hydraulic conductivity, ϕ is the soil porosity, θ_i is initial soil water
 219 content, d is the ponded water depth on the surface, ψ is the soil suction head at the wetting
 220 front, F is the accumulated infiltration volume during the rainfall event.

221 3.2.3 Hydrus-1D

222 Hydrus is a public domain Windows-based software that can simulate the movement of water,
 223 heat, and solute in variably saturated media. Two- and three-dimensional versions of also exist,
 224 but one-dimensional version of Hydrus-1D is more widely used in GR simulations. The
 225 governing equation in Hydrus-1D is the one-dimensional form of Richard's equation⁷³ (eq. 5):

$$226 \quad \frac{\partial \theta}{\partial t} = \frac{\partial}{\partial z} \left[K(\theta) \cdot \left(\frac{\partial h}{\partial z} + 1 \right) \right] \text{ eq. 5}$$

227 Where θ is the volumetric water content, $K(\theta)$ is the unsaturated hydraulic conductivity as a
 228 function of θ , z is the vertical coordinate, t is time and h is the hydraulic head.

229 The unsaturated soil hydraulic properties can be simulated with several analytical models in
 230 Hydrus-1D, in which the van Genuchten-Mualem method⁷⁴ is widely used to obtain the soil
 231 water retention curve and hydraulic conductivity function. The Van-Genuchten relationships
 232 can be written as:

$$233 \quad \theta(h) = \begin{cases} \theta_s & h \geq 0; \\ \theta_r + \frac{\theta_s - \theta_r}{[1 + (\alpha h)^n]^m} & h < 0 \end{cases} \quad \text{eq. 6}$$

$$234 \quad \theta_e = \frac{\theta - \theta_r}{\theta_s - \theta_r} \quad \text{eq. 7}$$

$$235 \quad K(\theta) = K_s \lambda \sqrt{S_e} \left[1 - \left(1 - S_e^{1/m} \right)^m \right]^2 \quad \text{eq. 8}$$

236 Where θ_s and θ_r are the saturated and residual water content; K_s is the saturated hydraulic
 237 conductivity, θ_e is the effective saturation; α , n , m ($1 - 1/n$) and λ (often assumed to be
 238 $0.5^{15,35,50,75}$) are fitting parameters of the soil water retention curve.

239 3.3 Water-leaving simulations

240 Water leaves GR through surface runoff, drainage mat flow and evapotranspiration. However,
 241 compared to simulating infiltration, these processes are not universal modeling considerations.
 242 Water-leaving simulations are model-specific. Therefore, in this section, we discuss the
 243 common modeling strategies to simulate drainage mat flow and evapotranspiration.

244 3.3.1 Drainage mat flow

245 Among the three models, only SWMM provides the capability to physically simulate bottom
 246 drainage. The water balance model may simulate drainage by adding a cascade reservoir model.
 247 In the SWMM modules, water percolates from the substrate into the drainage mat (f_p , eq. 9),
 248 described with Darcy's Law. Drainage mat flow is then simulated by using Manning's
 249 equations (q_1 , eq. 10); while, in bioretention module, it is simulated with an empirical power
 250 law (q_2 , eq. 11).^{40,76-79}

$$251 \quad f_p = K_s e^{HCO(\phi - \theta_t)} \quad \text{eq. 9}$$

252 Where HCO is a decay constant that describes hydraulic conductivity as a function of soil
 253 moisture content; θ_t is soil moisture content at time t .

$$254 \quad q_1 = \frac{W}{An_2} \sqrt{S} \phi_2 (d_2)^{\frac{5}{3}} \quad \text{eq. 10}$$

$$255 \quad q_2 = C_{3D} (d_3)^{\eta_{3D}} \quad \text{eq. 11}$$

256 Where n_1 and n_2 are the Manning's roughness for drainage mat, W is the width of the green
 257 roof, A is the area of the roof, d_2 is the depth of water in the drainage mat, S is the roof slope,
 258 ϕ_2 is the void ratio of drainage mat, C_{3D} is the underdrain discharge coefficient, d_3 is hydraulic
 259 head, η_{3D} is underdrain discharge exponent. It should be noted that d_3 is not limited to the total
 260 depth of storage unit, which can also be added by surface ponding.

261 3.3.2 Evapotranspiration

262 During event simulations, evapotranspiration (ET) is often neglected, because the ET rates are
 263 often assumed to be much smaller than precipitation.⁴⁷ However, ET is an important water
 264 budget term for long-term GR simulations, because it is the only way for GR to recover its
 265 retention capacity.⁸⁰ ET is difficult to directly measure, so it is often estimated based on two

266 widely used methods: the Hargreaves method⁸¹ (e.g., SWMM) (eq. 12) and the FAO-56
 267 Penman Monteith method⁸² (eq. 13), also known as potential ET and reference ET, respectively.
 268 Potential ET is a temperature-based estimate, while reference ET takes short grass as reference
 269 and includes meteorological data as an input to estimate ET.^{16,83,84} ET is divided, in Hydrus-
 270 1D, into evaporation and transpiration separately. Because none of the reviewed literature used
 271 Hydrus-1D to simulate ET, we do not discuss more detail.

272 Potential $ET = 0.0023 \cdot (0.48 \cdot R_a) \cdot (T_{mean} + 17.8) \cdot (T_{max} - T_{min})^{0.5}$ eq. 12

273 Reference $ET = \frac{0.408 \cdot (R_n - G) + \gamma \cdot \frac{900}{273 + T_{mean}} \cdot \mu_2 \cdot (e_s - e_a)}{\Delta + \gamma \cdot (1 + 0.34 \cdot \mu_2)}$ eq. 13

274 In these equations R_a is the daily total extraterrestrial radiation, T_{mean} is daily mean air
 275 temperature, T_{max} is daily maximum temperature, T_{min} is daily minimum temperature, R_n is
 276 net radiation at the crop surface, G is soil heat flux density, e_s is saturation vapor pressure, e_a
 277 is actual vapor pressure, γ is the psychrometric constant, μ_2 is daily average wind speed and Δ
 278 is slope of the vapor pressure curve.

279 4 Model practice

280 Building GR models requires data collection and parameter estimation. Calibrations were then
 281 often needed to adjust initial parameter estimates to improve model accuracy, by comparing
 282 predicted and measured outflow. This section discusses these model routines in practical
 283 applications. At the end of the section, we summarize model characteristics, capabilities, and
 284 potential applications (Table 3).

285 4.1 Model boundary conditions

286 Model boundary conditions include initial condition, upper boundary condition and lower
 287 boundary condition. The initial boundary condition is required for all the three models, which
 288 is often specified as the assumed or measured initial soil moisture content. Because Hydrus-1D
 289 numerically solves the partial differential equations, the upper and boundary conditions must
 290 be specified before running hydrus-1D simulations. The upper boundary is often assumed as a
 291 soil-atmosphere interface, with the surface flux equal to the rainfall input P .^{47,75} For lower
 292 boundaries, the free drainage condition and seepage condition are most commonly used in
 293 literature. The free drainage condition assumes the pressure head gradient is zero, corresponds
 294 to gravity flow; that is $\frac{\partial h}{\partial z} = -L$.^{18,50,73,85} The seepage boundary assumes that the flux
 295 remains zero as long as the boundary is unsaturated and the pressure head is set to zero once it
 296 is saturated^{14,47}, which means the outflow equals either to 0 or K_s .

297 4.2 Model parameterization

298 Common data used in GR modeling include rainfall, outflow, GR structural data and
 299 meteorological data (Table 1. Precipitation is the most important input for hydrological models,
 300 which is generally measured by rain gauge and is usually accessible to the public. Outflow is
 301 the output of GR models and its measurements are usually used to calibrate the models.
 302 However, outflow data may not be available for many modelers. Given limited funding, full-
 303 scale (building-scale) GRs may not exist in many cities. In addition, enabling outflow
 304 measurements in full-scale GRs often requires a systematic design prior to GR construction.
 305 For example, outflow from a GR in New York, USA was measured using Parshall flumes
 306 equipped with pressure transducers.⁸⁶ Another used a custom-designed weir device to measure

307 outflow.⁸⁷ In-pipe flow meters were installed to measure a GR's outflow in the city of Bologna,
 308 Italy.⁷⁹ Moreover, different outflow measurement methods have their own associated
 309 uncertainties, which also need to be accounted for when using them to evaluate or calibrate
 310 models. To solve this issue, substantial research effort has used pilot-scale experiments to
 311 mimic GR full-scale implementations, using the measured experimental outflow to build
 312 models.^{16,18,52,85}

313 To parameterize soil hydraulic properties, Hydrus-1D requires derivation of both a soil water
 314 retention curve and a hydraulic conductivity function (eq. 6 – eq. 8). These parameters can be
 315 derived from laboratory experiments such as with a pressure plate extractor^{16,18,75}, estimated
 316 using empirical functions⁵⁰, or via inverse solutions based on flow observations^{88,89}. Hydrus-
 317 1D also can be parameterized with estimates based on soil texture. However, the estimates in
 318 Hydrus-1D are limited to the abiotic soil texture classes based on percentiles of sand, silt and
 319 clay. Thus, these estimates may not be very useful in simulations, because GR substrate often
 320 includes organic matter to reduce substrate weight, increase porosity, and decrease bulk density
 321 characteristics^{47,84}. In addition, GR substrate, particularly for extensive GRs, often comprises
 322 of coarse and granular lightweight materials to reduce loading on the building roofs, which can
 323 differ substantially from the textures of natural soil.^{90,91} Further other additives, such as biochar,
 324 can be used to increase GR retention capacity⁸⁵. SWMM uses the Green-Ampt infiltration
 325 equation to simulate infiltration. Therefore, no experiments are needed to derive soil water
 326 retention curve and hydraulic conductivity function. Instead, a few soil physical parameters are
 327 specified, such as the saturated hydraulic conductivity and porosity.

328 **Table 1** Common data used for GR models

Data type	Objective	Common source	Model required	Data acquisition
Precipitation	Input	Rain gauge	Conceptual model/ mechanistic model	Easy
Temperature	ET estimates	Weather station	Continuous simulations	Easy
Solar radiation				
Vapor pressure				
Atmospheric pressure				
Outflow	Calibration/validation	Flow meter	Conceptual model/ mechanistic model	Difficult in full-scale measurements
Soil data	Parameterization of soil hydraulic properties	Lab experiments	Mechanistic model	Easy (water balance) Moderate (SWMM) Difficult (Hydrus-1D)
Roof dimensions	Model configuration	Field measurements	Conceptual model/ mechanistic model	Easy

329

330 Model parameterization depends on model structure complexity; a more complex model
 331 requires a larger number of parameters (Table 2. Some literature values and model
 332 recommended values are listed in the Table 2. The values of the soil hydraulic parameters for
 333 soil water retention curve and hydraulic conductivity function depend on specific soil textures.
 334 Accurate estimates are mainly derived through experimental measurements^{18,52}, so we did not
 335 summarize literature values for these in Table 2. Similarly, fitting values for water balance-
 336 based reservoir models were not included. Literature values are mainly related to SWMM
 337 model parameterization. Obviously, parameter values recommended by SWMM may differ

338 from values used in literature for specific simulations. For example, the saturated hydraulic
 339 conductivity values found in the literature (ranging between 2 – 1183 mm/hr) are substantially
 340 smaller than the values recommended by SWMM (1016 – 4064 mm/hr) (Table 2), which may
 341 suggest the permeability of engineered soils used in GR is deviated from natural soils.

342 Because model parameters may not be precisely estimated or directly measured, calibration is
 343 an important procedure to adjust parameter values. Calibration methods may include Bayesian
 344 algorithms³⁷, optimization techniques^{69,92,93}, or two-step calibration procedures^{41,94}. Prior to
 345 calibrating a model, parameter sensitivity analysis is a useful tool to understand the influence
 346 of parameters on model outputs and prioritize model parameters in model calibration. Common
 347 methods used to identify parameter sensitivity include one-factor-at-a-time^{93,94}, Bayesian
 348 uncertainty^{37,95} and global sensitivity analyses⁹⁶.

349 In reviewing parameter sensitivity analyses, we focused on the SWMM model, because it has
 350 a large number of parameters and the simplification of flow routing makes some parameters
 351 difficult/impossible to measure (such as parameters for the drainage mat). As various methods
 352 were used to evaluate parameter sensitivity, it is impossible to compare sensitivity indices
 353 across studies. Instead, we summarized the influential parameters identified by ten studies that
 354 conducted SWMM parameter sensitivity analysis^{34,37,50,69,78,86,92–94,96}. More specifically, we
 355 listed and counted the number of occurrences of the influential parameters identified in
 356 parameter sensitivity analysis (Table 2). For example, the substrate properties, such as porosity
 357 and field capacity, were identified 8 and 6 times, respectively, out of the 10 studies, and
 358 drainage mat properties, such as roughness (5 times), also have substantial effects on the
 359 outflow predictions.

360 **Table 2** Model parameters and associated parameter sensitivities (Blanks in the table means
 361 no available information or specific values; Y: required to specify; Sensitivity frequency*
 362 calculated as the counts of parameters identified as influential parameters by studies
 363 conducted parameter sensitivity analysis)

Parameters	SWM M BRC module	SWMM GR module	Richard's equation/ Hydrus-1D	Lumped Reservoir model	Default values (referring GR module)	Literature values	Sensitivit y frequency *
Surface roughness	Y					0.01 – 0.2	
Berm height (mm)	Y	Y			0 – 76.2	3 – 30	2
Surface void fraction	Y	Y			0.8 – 1.0	0.8 – 0.9	1
Slope (%)		Y				0.5 – 8	
Soil thickness (mm)	Y	Y	Y	Y	50.8 – 152.4	32 – 135	4
Porosity	Y	Y	Y	Y	0.45 – 0.6	0.39 – 0.7	8
Field capacity	Y	Y		Y	0.3 – 0.5	0.17 – 0.44	6
Wilting point	Y	Y			0.05 – 0.2	0.01 – 0.22	2
Initial moisture content	Y	Y	Y	Y			
Saturated hydraulic conductivity (mm/hr)	Y	Y	Y		1016 – 4064	2 – 1183	4
Wetting front suction head (mm)	Y	Y			50.8 – 101.6	6 – 100	1
Decay constant	Y	Y			30 – 55	5 – 50	6
Storage layer (drainage mat) thickness (mm)	Y	Y			12.7 – 50.8	3.8 – 76.2	2
Storage void (drainage	Y	Y			0.2 – 0.4	0.01 – 0.98	2

mat) fraction							
Drainage mat roughness	<i>Y</i>				0.01 – 0.03	0.01 – 0.4	5
Drain coefficient (mm/h)		<i>Y</i>				2.1 – 8.4	
Drain exponent		<i>Y</i>				0.5 – 2.1	
Soil residual water contents			<i>Y</i>				
Saturated water content			<i>Y</i>				
α (fitting parameter)			<i>Y</i>				
n (fitting parameter)			<i>Y</i>				
λ (fitting parameter)			<i>Y</i>				
k (fitting parameter)				<i>Y</i>			
φ (fitting parameter)				<i>Y</i>			
Total number of parameters	14	15	9	7			

364

365 Even though the initial soil moisture is considered as the initial condition rather than as a
366 parameter, it has significant effects on event-based simulations^{76,77,79,94} It reflects the degree to
367 substrate initially filled with water.⁷⁶ In general, the lower initial soil moisture, the smaller the
368 runoff volume and peak rate and the longer the peak delay will be^{15,69}. In addition, soil water
369 percolation is often assumed to be triggered when the soil moisture content exceeds field
370 capacity^{33,54,97}. An initial water content at field capacity can lead to instant drainage flow even
371 at the beginning of an event^{78,94}. Therefore, the initial soil moisture should be carefully specified
372 in simulations. The initial moisture content can be specified by using moisture sensor^{33,69,97} or
373 assumed by modelers⁸⁷.

374 Considering data acquisition and parameter estimation, several things emerge from the
375 reviewed literature:

- 376 (1) Outflow measurements are often unavailable, because 1) an existing built GR is the
377 prerequisite to measure in-site outflow; and 2) the setup of outflow measurement is
378 complex. Many GR models, thus, were built using experimental data.
379 (2) little data are needed to parameterize soil hydraulic properties for water-balance
380 models, but the routing parameters requires calibration.
381 (3) SWMM has the largest number of parameters to specify (>10), but it can explicitly
382 simulate flow through the entire vertical profile. Parameter values can be easily found
383 from literature or assumed.
384 (4) Soil parameters in Hydrus-1D often require large efforts of laboratory measurements
385 or model calibrations.

386 4.3 Model potential application

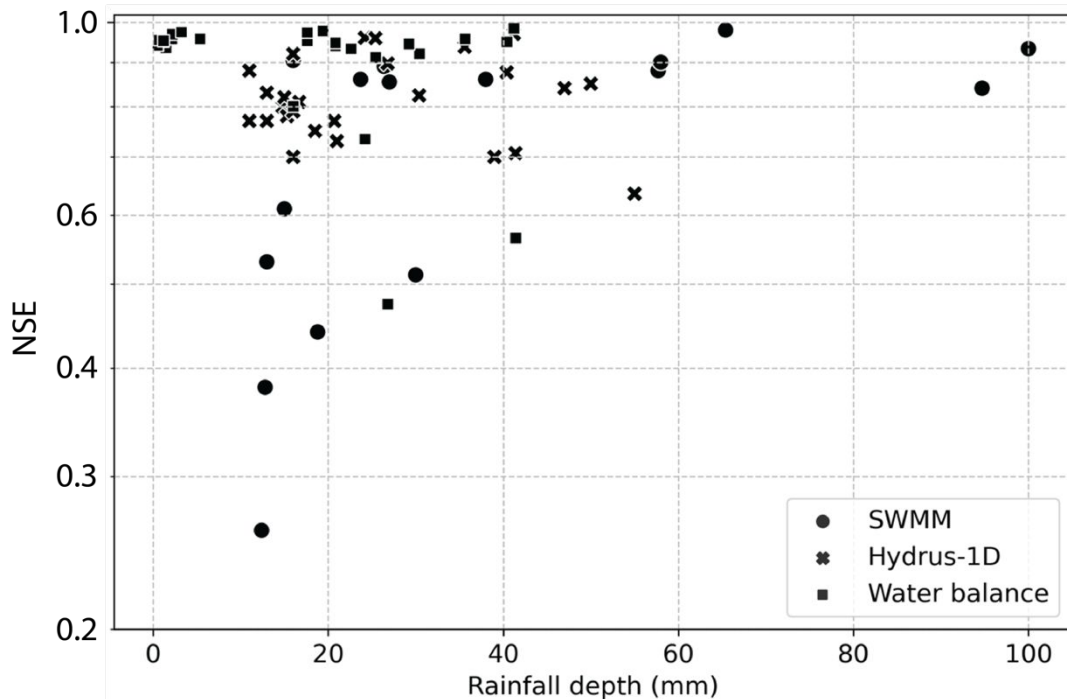
387 (1) Model evaluation

388 To evaluate model performance, several metrics have been used in the literature. Among these
389 evaluations, Nash-Sutcliffe efficiency is widely used (NSE, eq. 14), which measures the
390 goodness of fit between model predictions and observations (closer to 1, better simulations)⁹⁸.
391 To define acceptable model performance, several studies suggest a threshold of NSE >
392 0.5^{41,70,78}. Although comparing NSE values across models constructed at different sites (Fig. 2)
393 may not be a good way to compare model performance because of their varying climate
394 conditions and input data, a naïve comparison can still show some aspects of the ability of a

395 model to replicate measured outflow. Based on Fig. 2, all three models can generate good
 396 predictions of GR outflow. For the majority of all events (90%), the NSE is > 0.5. SWMM
 397 seems to show greater variability in predictions with a larger portion (28%) of events with NSE
 398 < 0.5 than the other two models. Furthermore, NSE evaluations for SWMM present a degree
 399 of correlation to event depths, with NSE values more likely to be > 0.5 when larger events are
 400 simulated (depths > 20 mm).

$$401 \quad NSE = 1 - \frac{\sum_{i=1}^n (Q_{o,i} - Q_{s,i})^2}{\sum_{i=1}^n (Q_{o,i} - \overline{Q_o})^2} \text{ eq. 14}$$

402 Where $Q_{o,i}$ and $Q_{s,i}$ are the observed and simulated flow discharge values, respectively; $\overline{Q_o}$ is
 403 the observed mean flow.



404

405 **Fig. 2** Comparison of NSE and rainfall depth (mm) in GR outflow event-based simulations
 406 based on the reviewed studies evaluating model performance.^{14,34,47,70,93}

407 Two model evaluation strategies are often considered. The first strategy is selecting rainfall
 408 events observed at the same site, which is a commonly used method^{18,35,36,47}. In general, so-
 409 called validated models perform more poorly than calibrated models, because calibration
 410 involves optimizing model performance by finding the parameter values that lead to best-fit
 411 outputs^{18,34–36,78,92,94}. The second strategy is cross-validation, in which models are tested among
 412 different sites and climate forcings^{41,56,58}. This strategy is becoming increasingly popular,
 413 because it is important for GR planning that the model can predict the performance of new
 414 implementations when data are unavailable. Nevertheless, the transferred model often fails to
 415 predict GR outflow at different sites^{56,58}. The reasons for this failure are associated with the
 416 uncertainties in model physical characterization and parameterization, which will be discussed
 417 in more detail in Section 5.

418 (2) Model applications

419 One goal of GR modeling is characterization of GR performance under various designs and
 420 climate forcings. Although the three models can replicate GR outflow, Hydrus-1D can simulate
 421 unsaturated flow processes based on water retention curve and hydraulic conductivity function,
 422 which are essential to clarify soil hydraulic properties. Therefore, Hydrus-1D can be used to
 423 experimentally simulate the effects on substrate compositions on GR detention.^{52,91} For
 424 example, Huang et al. (2020) explored the effects of biochar addition on soil hydraulic
 425 properties.⁸⁸ They found biochar-amendments increased the retention capacity and detention
 426 capacity but decreased saturated hydraulic conductivity because of the rough surface of biochar.
 427 That said, large data demands on model parameterization and high computational costs may
 428 limit Hydrus-1D applications to situations where soil hydraulic properties are vital to render.

429 Another goal of GR modeling is to explore the watershed/citywide effects of GR
 430 implementation scenarios on stormwater reduction. GR models are commonly integrated into
 431 watershed hydrological models.^{37,40,70,99} Thus, a simple model that can be easily built and
 432 incorporated into watershed models will provide more modeling flexibility. In these cases,
 433 many current large-scale simulations rely on the use of SWMM.^{37,40,69,70} Using SWMM 1)
 434 model parameters can be easily found or calibrated; 2) SWMM GR module and bioretention
 435 modules have full capacity to physically simulate the entire water circle with GR; 3) GR
 436 simulations can be easily incorporated into SWMM stormwater model network.

437 The three GR models have specific strengths and shortcomings, so model selections and
 438 applications depend on available data and research question. If monitored outflow data are
 439 available to calibrate GR model, the water balance model is a good option, because it can
 440 generate accurate simulation results (Fig. 2) with low computational demands^{29,33,63,100}.
 441 However, conceptual models such as the lumped reservoir model may have more uncertainties
 442 in flow predictions relative to mechanistic models because their simple model structures cannot
 443 reflect soil water transport dynamics.³⁷ Further, without explicit parametrization of soil
 444 properties, the water-balance model is often case-specific.⁶³ In contrast, SWMM and Hydrus-
 445 1D both explicitly parameterize soil water transport processes, which can better interpret soil
 446 water transport processes. Benefits from numerically solving Richard's equation, Hydrus-1D
 447 is capable to be used to explore soil hydraulic properties. However, considering the ease of data
 448 collection and parameter estimation, SWMM could be more applicable than Hydrus-1D, since
 449 parameter values can be gathered from the literature. A summary of the potential model
 450 practical uses is shown in Table 3.

451 **Table 3** The main characteristics and capabilities of GR models

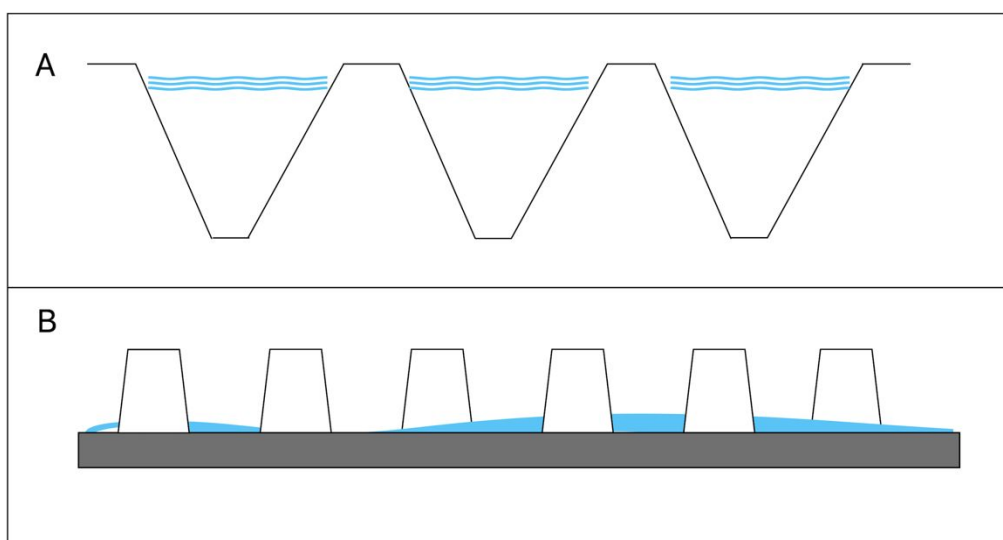
Model types	Characteristics	Capabilities	Potential applications
Water balance	<i>Type:</i> conceptual model <i>Development:</i> water fluxes based on water balance and often combined with lumped reservoir models. <i>Computational cost:</i> low	Water storage; Infiltration; Drainage flow; ET	Outflow simulations
SWMM	<i>Type:</i> mechanistic model <i>Development:</i> Green-Amp infiltration equation, Manning' equation and empirical power law <i>Computational cost:</i> moderate	Water storage; Infiltration; Drainage flow; ET	Outflow simulations; Full vertical profile flow simulations; Large-scale simulations;
Hydrus-1D	<i>Type:</i> mechanistic model <i>Development:</i> Richard's equation <i>Computational cost:</i> high	Water storage; Infiltration; ET	Outflow simulations; Understanding substrate hydraulics

452 5 Limitations and challenges for GR model applications

453 Although the reviewed studies contributed to GR model development, some critical issues may
 454 continue to limit model applications. For example, model parameter transferability is very low
 455 among different models at same sites or the same models at different sites^{37,40,41,86}.
 456 Discrepancies in the calibrated model parameters raise concerns about the accuracy and
 457 reliability of GR models as a design tool. Therefore, identifying the limitations of existing
 458 models is important for improving future models. In this section, four key challenges in GR
 459 model development are identified, including modeling drainage mat flow, characterization of
 460 soil hydraulic properties, ET estimates and scale effects on GR simulations.

461 5.1 Uncertainties in drainage mat flow

462 The drainage mat (bottom layer) temporarily stores and gradually drains excess water from the
 463 system to enhance detention (Fig. 3).⁷⁸ **Fig. 3** Current GR studies mainly focus on extensive
 464 GRs, with a depth of substrate less than 15 cm, in which the substrate void volume can be
 465 quickly filled, resulting in a fast drainage response.³⁴ Parameterization of the drainage mat,
 466 therefore, plays a significant role in successful replication of observed outflow in extensive
 467 GR.^{34,41,67,76,78,92} However, the detention of a drainage mat is rarely understood and physically
 468 simulated. Most GR models, such as hydrus-1D and water-balance models, lack the ability to
 469 simulate drainage mat flow. Those models that did not include drainage mat simulations often
 470 used conceptual reservoir models to simulate the effects of drainage mat on water detention.⁹⁷
 471 Palla, Gnecco, and Lanza (2012) connected two linear reservoirs to simulate water moving
 472 through the substrate and drainage mat respectively, in which the second layer (assumed as a
 473 drainage mat) took the output from the first layer (assumed as the soil medium) as input to
 474 simulate the drainage.⁴⁷ Vesuviano, Sonnenwald, and Stovin (2014) modelled GR by
 475 connecting two nonlinear reservoirs in series, which inflow to the drainage layer being equal to
 476 the outflow from the substrate.⁶⁵ However, the lumped model aims to replicate the drainage
 477 flow but lacks physical interpretations on the associated routing parameters for the drainage
 478 mat, which cannot link back to the model to physically interpret the effects of shape or material
 479 of drainage mat on GR outflow.



480

481 **Fig. 3** Schematic examples of drainage mat with temporary storage (A) and without

482 temporary storage (B)

483 Of the reviewed models, only the SWMM model explicitly incorporates drainage mat flow
484 simulations in the GR and bioretention cell modules. Regardless of the routing assumptions in
485 the two SWMM modules, the main physical difference between them is the roof slope
486 characterization. The SWMM GR module utilizes Manning's equation, in which the roof slope
487 can be explicitly parameterized. However, when a flat roof is simulated with the slope set to
488 zero, the assumption of uniform open channel flow based on Manning's equation is violated,
489 corresponding to instantaneous runoff.^{54,78} In contrast, a drainage layer in the bioretention
490 module is modeled with an empirical power law (assuming a slope of 0), which can be
491 interpreted as an orifice equation.⁷⁶ Jeffers et al. (2022) evaluated the effectiveness of the two
492 modules to simulate GR outflow with different slopes and they found the bioretention cell
493 module is more accurate to replicate flow in flat roof simulations.⁷⁸ However, they did not
494 deduce an optimal module to parameterize and simulate the drainage mat flow.

495 5.2 Representation of soil characteristics

496 Parameterization of soil characteristics is crucial to precisely model water movement in the GR
497 substrate.^{87,92–94,96,101} In many cases, the simple conceptual model only obtains a robust
498 representation of the hydraulic behavior of GR and does not derive an accurate representation
499 of soil physics. Therefore, compared to the mechanistic model, fitted parameters of the
500 conceptual model cannot be transferred to models built at different sites.⁶³

501 In mechanistic model applications, calibrated values of soil parameters are often used to
502 estimate soil hydraulic characteristics when soil experiments are unavailable.^{14,15,35,47,75}
503 However, sometimes model calibration is only based on the goodness of fit of outflow
504 simulations and the calibrated parameters do not necessarily correspond to the actual soil
505 properties.^{37,41,93,94} Broekhuizen et al. (2021) compared four models – SWMM, Hydrus-1D,
506 Mike-SHE and Urbis – and found low consistency of soil parameter values across models after
507 calibration, which raises questions about the generalizability of soil parameterization on model
508 applications.³⁷ Jeffers et al. (2022) found the calibrated hydraulic conductivity slopes
509 (equivalent to the decay constant in eq. 9) were different between SWMM modules, with values
510 of 20 and 51, respectively, for the bioretention cell module and GR module.⁷⁸ As a result, a
511 non-representative set of soil parameters with low transferability inevitably led to unreliable
512 modelling results when the model was applied to different sites and scales.^{40,86,102}

513 Further, the substrate properties are influenced by vegetation^{14,75,97}, resulting in field substrate
514 characteristics that may not match the results from laboratory soil tests¹⁰². Johannessen et al.
515 (2019) found laboratory measured porosity was higher than calibrated porosity⁴¹, possibly due
516 to cracks generated by vegetation roots development⁸⁵. They also found the wilting points were
517 lower in lab measurements. This may be due to the wilting point being plant-specific — for
518 example, drought-tolerant vegetation planted in GR can resist wilting, which leads to higher
519 retention capacity than bare soil⁸⁷. In a SWMM simulation, Hamouz and Muthanna (2019) used
520 laboratory measured porosity and hydraulic conductivity to simulate GR outflow, but could not
521 successfully replicate the outflow.⁹³

522 Last, soil hydraulic properties may change over time due to substrate aging and changes in soil
523 water condition. An experiment conducted by Bouzouidja et al. (2018) that monitored the aging
524 of substrate suggested the saturated water content decreased by 4% and the saturated hydraulic
525 conductivity increased by 22%, after three years exposure of substrate.³⁹ Starry et al. (2016)

526 found the substrate field capacity was related to antecedent soil water conditions in the
527 substrate.³³ Sims et al. (2019) assigned different values to field capacity (with 0.215 for the wet
528 periods and 0.193 for drier period) and achieved good predictions even without model
529 calibration.¹⁰³

530 5.3 Evapotranspiration estimates

531 Unlike other GI techniques with deeper soil that rely on infiltration as the primary water
532 retention mechanism, GR retains water within the shallow substrate and then recovers its
533 retention capacity via ET over dry weather days. Therefore, the water retention performance of
534 GR is positively related to soil water storage capacity and ET¹⁰⁴.

535 In the literature, potential ET (Hargreaves method) and reference ET (FAO-56 Penman
536 Monteith method) are mostly used to estimate ET, but many studies found these two approaches
537 may not appropriately estimate actual ET because actual ET is not only influenced by climate
538 conditions but also by vegetation type and soil moisture content.^{16,40,70,79,80,87,92,94,96} Poë, Stovin,
539 and Berretta (2015) found a declining ET occurred when the soil moisture availability was
540 reduced and an increased ET (by 17% in spring and 23% in summer) in substrate with addition
541 of vegetation compared to bare soil.¹⁰⁵ Similar findings were observed by Harper et al. (2015)
542 that when the plants were dormant over winter, variation of ET between the planted and
543 unplanted substrate trays was small.⁸ However, potential ET and reference ET models do not
544 include parameters to capture the effects of vegetation and soil water availability.

545 To capture the influence of soil moisture on ET estimates, in a simple manner, monthly soil
546 recovery patterns were used to modify the estimated ET^{41,79}. However, one drawback of this
547 modification is it requires calibration and thus does not necessarily indicate the actual soil water
548 availability.⁴¹ As a result, more complex modifications were explored to explicitly account for
549 the influence of soil water availability, for example modifications based on the dry period
550 duration^{36,94} or soil moisture time series^{16,71,86}.

551 To capture the influences of vegetation type on ET, the reference ET is multiplied by a crop
552 coefficient to account for the physiological influence of different types of vegetation on ET
553 ^{16,33,92}. However, this approach was initially developed for agricultural applications and the crop
554 coefficients are not well-defined for green roof species and often unavailable to be used for GR
555 modeling or design³³. In GR literature, common plants can be classified as C₃ plants and
556 Crassulacean Acid Metabolism (CAM) vegetation. C₃ plants are characterized by C₃
557 metabolisms, in which the CO₂ is fixed into a compound with three carbon atoms.¹⁰⁶ C₃ plants,
558 including lawn grasses and herbs, usually have a high water demand and show high ET rates
559 but these plants can require irrigation in drought areas.¹⁰⁶ CAM vegetation, such as *Sedum*
560 species, can absorb CO₂ in the night and usually do not require irrigation, and have relatively
561 low ET rates.^{92,107} Cristiano et al. (2020) found that high water demand species such as C₃ plants
562 could have higher ET rates with a crop coefficient > 1, which results in a higher retention
563 capacity due to its higher probability to have low antecedent soil moisture at the beginning of
564 rainfall events.¹⁰⁶ Based on the literature, crop coefficients were summarized in Table 4. The
565 crop coefficients are seasonal and species-specific, and high water-demand species can have
566 crop coefficients larger than 1. However, there are still limited data reported on crop coefficients
567 for GR plant species. Therefore, more studies are needed to investigate crop coefficients for
568 different species and provide reference values for GR modeling and design.

569

570

Table 4 Summary of different crop coefficients used in GR modeling

Study	Locations	Plant species	Crop coefficients
Sherrard and Jacobs (2012) ¹⁹	New Hampshire, US	Sedum species	0.53
Berretta, Poë, and Stovin (2014) ¹⁶	Sheffield, UK	Sedum species	0.65 – 1.36, substrate specific
Cristiano et al. (2020) ¹⁰⁶	Cagliari, Italy	Several American Agave plants	0.5
Starry et al. (2016) ³³	Maryland, US	Sedum species	0.21 – 0.71, species and seasonal specific
Locatelli et al. (2014) ⁶³	Copenhagen and Odense, Denmark	Sedum species	0.89–0.95
Szota et al. (2017) ¹⁰⁷	Melbourne, Australia,	High water use plants	1.16 – 1.67, species specific
Szota et al. (2017) ¹⁰⁷	Melbourne, Australia,	Low water use plants	0.59 – 0.97, species specific

571

572 5.4 Scale effects on GR simulations

573 Many GR simulations depend on data measured from pilot-scale experiments, because pilot-
574 scale GR can be easily accessed and monitored¹⁰⁸. For example, drainage in pilot-scale GR can
575 be easily observed by installing rain barrels under the test beds to measure water level^{63,68,92}.
576 However, because pilot-scale GR is often built on elevated test beds above the roof
577 base^{76,92,95,103}, it suffers from the exposure to additional heat at the bottom which can lead to
578 higher soil water loss^{79,109}. In contrast, the full-scale GR is installed directly on the rooftop and
579 can contain non-vegetated areas^{77,86}, so the combined total flow of bottom drainage and
580 overland flow eventually discharges into the local sewer^{40,79,86}, even though the surface flow
581 may contribute a small portion to the total flow³⁵. Drainage monitoring in full-scale GR is
582 complex and depends on the presence and design of roof drains.⁸⁶ Possible monitoring
583 strategies include use of flow meters or water level sensors installed in either GR drainage
584 channels^{48,86} or downspouts⁷⁹.

585 Researchers and stormwater managers who pursue GR implementations to address stormwater
586 issues need simulations of GR city-level performance to support their decision-making.
587 Considering the differences in runoff routing and monitoring between pilot-scale GR and full-
588 scale GR, it is unclear whether GR models based on pilot-scale experiments are representative
589 of full-scale GR implementations for stormwater management⁷⁹. Further, city-level
590 performance is often simulated by creating roof retrofitting scenarios. These scenarios are
591 defined based on spatial analyses to identify potential roof areas and assume different
592 percentages of grey roof to be replaced with GR⁷⁰. However, the city-level performance of GR
593 could also be influenced by the GR spatial distributions. Versini et al. (2016) identified that the
594 distribution of roofs, locating them upstream or downstream of the catchment, impacted
595 stormwater runoff delay.⁶² They also found GR implementations in the upstream of the
596 catchment could better delay runoff. Therefore, modeling city-level performance of GR
597 requires further considerations to define scenarios that render GR designs, intrinsic catchment
598 characteristics, and GR spatial distributions. Finally, in addition to understanding the large-
599 scale effects of GR implementation, investment costs can be a significant concern for the
600 practical application of GR. In the reviewed literature, only three studies^{86,106,110} included a cost-
601 effectiveness analysis in their simulations. Their results suggest cost-effective stormwater

602 management using GR should consider attentively the designs (such as soil and plants) and
603 potential implementation locations. Given limited funding, the ability to realize potential
604 benefits through practical uses still needs to be comprehensively evaluated.

605 **6 Future needs**

606 6.1 GR monitoring to improve model validation

607 GR models need to be validated to improve model predictions in an urban landscape,
608 particularly for models built based on pilot-scale experiments. Considering the possible
609 inconsistent values of soil parameters between measurements and model calibrations,
610 uncertainty and variability among different model types could be reduced with more field
611 monitoring to support understanding of GR performance. Therefore, building more monitoring
612 programs can help improve understanding of the changing/aging effects of soil properties on
613 water transport. Installing sensors, such as moisture sensors, could facilitate monitoring,
614 because they can continuously track soil water conditions and provide insights to detect
615 potential changes in soil hydraulic properties.

616 6.2 Deriving actual ET for GR systems

617 Currently, most common ET predictive methods do not properly predict GR ET. GR managers
618 could consider different types of plants under different climate regimes. Pilot-scale studies need
619 to be expanded to derive crop coefficients for various GR plant types to estimate actual ET and
620 inform future GR design. Soil moisture conditions can impact GR ET. Further research is
621 needed to improve ET estimates under water stress conditions and provide reasonable estimates
622 of the soil moisture levels that significantly impact actual ET in GR systems.

623 6.3 Characterization of GR components

624 Further studies are needed to characterize the effects of plants, soil, and drainage mat on GR
625 hydrological modeling. The interception GR plants can serve to store and return rainfall to the
626 atmosphere through evaporation. For example, a mean initial abstraction varying from 5 mm
627 to 5.9 mm was reported in a previous GR study.⁵⁵ To expand current soil column experiments⁵²,
628 adding a commercial vegetation mat atop the soil may help to explore the effects of plant
629 interception. Considering the granular difference between GR substrate and natural soil,
630 conventional models describing soil water characteristic curves and hydraulic conductivity
631 functions need to be evaluated with various substrate types by fitting experimental data to
632 improve substrate physical representation and model transferability. Further observations of
633 outflow from full-scale GRs are recommended to determine the impact of GR geometry and
634 drain placement on GR detention.

635 6.4 City-scale performance evaluation

636 More holistic GR simulations at the city scale could be very helpful to support decision-making.
637 Current city-scale GR simulations mainly focus on evaluating stormwater runoff reductions.
638 Broader hydrological benefits associated with GR implementations, such as combined sewer
639 overflow reductions, need to be evaluated to provide a better understanding of city-scale GR
640 performance. Moreover, identifying potential GR siting locations in scenario simulations can
641 be influenced by many factors, e.g., roof slopes and building functions. Use of rooftop maps
642 alone can overestimate GR siting potentials. To better identify all potential GR spatial
643 distributions, rigorous land use analysis is needed with consideration of the comprehensive
644 general city plan. Last, to better understand city-level performance of GR, studies on
645 optimization of GR designs and placements incorporating cost and benefit analysis are
646 suggested to provide insights to stormwater managers regarding the incorporation of GR into
647 stormwater management.

648 **7 Conclusion**

649 Existing efforts to model GR can be classified as conceptual models and mechanistic models.
650 Both models can predict GR outflow^{14,47}. Compared to mechanistic models, conceptual models
651 are simple and require low computational costs. However, due to lack of physical meaning of
652 the routing parameters, conceptual models are often case-specific⁶³ and the results usually
653 cannot be generalized. SWMM and Hydrus-1D both explicitly parameterize soil water transport
654 processes. By solving Richard's equation, Hydrus-1D is able to simulate flow through
655 unsaturated soil and, therefore, provide understanding of soil hydraulic properties, but it
656 requires substantial effort to derive soil parameters. SWMM has a large number of parameters
657 to specify (>10), but it has full capacities to simulate flow through the entire GR vertical profile.
658 In addition, SWMM GR models can be easily incorporated into SWMM stormwater model
659 framework, so it is widely used to simulate the large-scale effects of GR implementations.
660 Considering the limitations in model applications, efforts are still needed to improve model
661 accuracy, by better parameterizing drainage mat flow, estimating evapotranspiration,
662 characterizing soil properties and conducting monitoring programs. To promote GR
663 implementation, comprehensive studies are required to illuminate trade-offs between the cost
664 of GR placement/retrofit and the resulting flow reductions.

665 **Conflicts of interest**

666 The authors have no competing interests to declare.

667 **Acknowledgements**

668 This work is supported by the National Science Foundation, USA under Grant No. 1854827.

669 **Authors Contributions**

670 Zhaokai Dong: investigation, reviewed literature, designed review process, wrote manuscript.

671 Daniel A Bain: edited manuscript, provided guidance on content.

672 Kimberly A Gray: edited manuscript, provided guidance on content.

673 Murat Akcakaya: edited manuscript, provided guidance on content.

674 Carla Ng: funding acquisition, resources, supervision, edited manuscript

675 **Notes and references**

676

- 677 1 C. L. Arnold and C. J. Gibbons, Impervious surface coverage: the emergence of a key
678 environmental indicator, *Journal of the American Planning Association*, 1996, **62**, 243–
679 258.
- 680 2 T. R. Schueler, L. Fraley-McNeal and K. Cappiella, Is impervious cover still important?
681 Review of recent research, *J. Hydrol. Eng.*, 2009, **14**, 309–315.
- 682 3 H. Li, L. J. Sharkey, W. F. Hunt and A. P. Davis, Mitigation of impervious surface
683 hydrology using bioretention in north carolina and maryland, *J. Hydrol. Eng.*, 2009, **14**,
684 407–415.
- 685 4 J. Marsalek, *Urban water cycle processes and interactions*, CRC Press, 2014.
- 686 5 L. S. Coffman, R. Goo and R. Frederick, Low-impact development: an Innovative
687 alternative approach to stormwater management, *WRPMD '99: Preparing for the 21st*
688 *Century*, 1999, 1–10.
- 689 6 J. Zischg, B. Rogers, A. Gunn, W. Rauch and R. Sitzenfrei, Future trajectories of urban
690 drainage systems: A simple exploratory modeling approach for assessing socio-technical
691 transitions, *Science of The Total Environment*, 2019, **651**, 1709–1719.
- 692 7 Y. Her, J. Jeong, J. Arnold, L. Gosselink, R. Glick and F. Jaber, A new framework for
693 modeling decentralized low impact developments using Soil and Water Assessment Tool,
694 *Environmental Modelling & Software*, 2017, **96**, 305–322.
- 695 8 G. E. Harper, M. A. Limmer, W. E. Showalter and J. G. Burken, Nine-month evaluation of
696 runoff quality and quantity from an experiential green roof in Missouri, USA, *Ecological*
697 *Engineering*, 2015, **78**, 127–133.
- 698 9 Center for Neighborhood Technology (CNT), *The value of green infrastructure, A guide*
699 *to recognizing its economic, environmental and social benefits*, 2010.
- 700 10 L. S. H. Lee and C. Y. Jim, Thermal-cooling performance of subtropical green roof with
701 deep substrate and woodland vegetation, *Ecological Engineering*, 2018, **119**, 8–18.
- 702 11 Green Roofs for Healthy Cities, *2019 annual green roof industry survey: executive*
703 *summary*, 2019.
- 704 12 R. Berghage, D. Beattie, A. Jarrett, C. Thurig, F. Razaeei and T. O'Connor, *Green roofs for*
705 *stormwater runoff control*, U.S. Environmental Protection Agency, Washington, DC.,
706 2009.
- 707 13 L. Kosareo and R. Ries, Comparative environmental life cycle assessment of green roofs,
708 *Building and Environment*, 2007, **42**, 2606–2613.
- 709 14 K. X. Soulis, J. D. Valiantzas, N. Ntoulas, G. Kargas and P. A. Nektarios, Simulation of
710 green roof runoff under different substrate depths and vegetation covers by coupling a
711 simple conceptual and a physically based hydrological model, *Journal of Environmental*
712 *Management*, 2017, **200**, 434–445.
- 713 15 R. Castiglia Feitosa and S. Wilkinson, Modelling green roof stormwater response for
714 different soil depths, *Landscape and Urban Planning*, 2016, **153**, 170–179.
- 715 16 C. Berretta, S. Poë and V. Stovin, Reprint of “Moisture content behaviour in extensive
716 green roofs during dry periods: The influence of vegetation and substrate characteristics”,
717 *Journal of Hydrology*, 2014, **516**, 37–49.
- 718 17 L. Bengtsson, L. Grahn and J. Olsson, Hydrological function of a thin extensive green roof
719 in southern Sweden, *Hydrology Research*, 2005, **36**, 259–268.
- 720 18 J. Wang, A. Garg, N. Liu, D. Chen and G. Mei, Experimental and numerical investigation
721 on hydrological characteristics of extensive green roofs under the influence of rainstorms,
722 *Environ Sci Pollut Res*, , DOI:10.1007/s11356-022-19609-w.
- 723 19 J. A. Sherrard and J. M. Jacobs, Vegetated roof water-balance model: experimental and
724 model results, *J. Hydrol. Eng.*, 2012, **17**, 858–868.
- 725 20 Doug Banting, Hitesh Doshi, James Li, and Paul Missios, *Report on the environmental*
726 *benefits and costs of green roof technology for the city of toronto*, Ryerson University,
727 2005.

- 728 21 K. L. Getter, D. B. Rowe and J. A. Andresen, Quantifying the effect of slope on extensive
729 green roof stormwater retention, *Ecological Engineering*, 2007, **31**, 225–231.
- 730 22 D. Hutchinson, P. Abrams, R. Retzlaff and T. Liptan, *Stormwater monitoring two ecoroofs*
731 *in portland, Oregon, USA*, 2003.
- 732 23 J. Mentens, D. Raes and M. Hermy, Green roofs as a tool for solving the rainwater runoff
733 problem in the urbanized 21st century?, *Landscape and Urban Planning*, 2006, **77**, 217–
734 226.
- 735 24 D. J. Bliss, R. D. Neufeld and R. J. Ries, Storm water runoff mitigation using a green roof,
736 *Environmental Engineering Science*, 2009, **26**, 407–418.
- 737 25 T. Carter and C. R. Jackson, Vegetated roofs for stormwater management at multiple
738 spatial scales, *Landscape and Urban Planning*, 2007, **80**, 84–94.
- 739 26 A. C. Moran, W. F. Hunt and J. T. Smith, Green roof hydrologic and water quality
740 performance from two field sites in north carolina, *Managing Watersheds for Human and*
741 *Natural Impacts*, 2005, 1–12.
- 742 27 T. Liptan and R. K. Murase, Watergardens as stormwater infrastructure in Portland,
743 Oregon, *Handbook of water sensitive planning and design*, 2002, 125–154.
- 744 28 F. Viola, M. Hellies and R. Deidda, Retention performance of green roofs in representative
745 climates worldwide, *Journal of Hydrology*, 2017, **553**, 763–772.
- 746 29 A. Talebi, S. Bagg, B. E. Sleep and D. M. O’Carroll, Water retention performance of green
747 roof technology: A comparison of canadian climates, *Ecological Engineering*, 2019, **126**,
748 1–15.
- 749 30 B. G. Johannessen, H. M. Hanslin and T. M. Muthanna, Green roof performance potential
750 in cold and wet regions, *Ecological Engineering*, 2017, **106**, 436–447.
- 751 31 F. Bettella, V. D’Agostino and L. Bortolini, Drainage flux simulation of green roofs under
752 wet conditions, *J Agricult Engineer*, 2018, **49**, 242–252.
- 753 32 M. Hardin, M. Wanielista and M. Chopra, A mass balance model for designing green roof
754 systems that incorporate a cistern for re-Use, *Water*, 2012, **4**, 914–931.
- 755 33 O. Starry, J. Lea-Cox, A. Ristvey and S. Cohan, Parameterizing a water-balance model for
756 predicting stormwater runoff from green roofs, *J. Hydrol. Eng.*, 2016, **21**, 04016046.
- 757 34 X. Haowen, W. Yawen, W. Luping, L. Weilin, Z. Wenqi, Z. Hong, Y. Yichen and L. Jun,
758 Comparing simulations of green roof hydrological processes by SWMM and HYDRUS-
759 1D, *Water Supply*, 2020, **20**, 130–139.
- 760 35 W.-Y. Yang, D. Li, T. Sun and G.-H. Ni, Saturation-excess and infiltration-excess runoff
761 on green roofs, *Ecological Engineering*, 2015, **74**, 327–336.
- 762 36 A. Palla, I. Gnecco and P. La Barbera, Assessing the hydrologic performance of a green
763 roof retrofitting scenario for a small urban catchment, *Water*, 2018, **10**, 1052.
- 764 37 I. Broekhuizen, S. Sandoval, H. Gao, F. Mendez-Rios, G. Leonhardt, J.-L. Bertrand-
765 Krajewski and M. Viklander, Performance comparison of green roof hydrological models
766 for full-scale field sites, *Journal of Hydrology X*, 2021, **12**, 100093.
- 767 38 G. Ercolani, E. A. Chiaradia, C. Gandolfi, F. Castelli and D. Masseroni, Evaluating
768 performances of green roofs for stormwater runoff mitigation in a high flood risk urban
769 catchment, *Journal of Hydrology*, 2018, **566**, 830–845.
- 770 39 R. Bouzouidja, G. Séré, R. Claverie, S. Ouvrard, L. Nuttens and D. Lacroix, Green roof
771 aging: Quantifying the impact of substrate evolution on hydraulic performances at the lab-
772 scale, *Journal of Hydrology*, 2018, **564**, 416–423.
- 773 40 P.-A. Versini, D. Ramier, E. Berthier and B. de Gouvello, Assessment of the hydrological
774 impacts of green roof: From building scale to basin scale, *Journal of Hydrology*, 2015, **524**,
775 562–575.
- 776 41 B. G. Johannessen, V. Hamouz, A. S. Gagne and T. M. Muthanna, The transferability of
777 SWMM model parameters between green roofs with similar build-up, *Journal of*
778 *Hydrology*, 2019, **569**, 816–828.
- 779 42 Yanling Li and Roger W. Babcock Jr, Green roof hydrologic performance and modeling:
780 a review, *Water Science and Technology*, 2014, **69**, 727–738.
- 781 43 K. Zhang and T. F. M. Chui, A review on implementing infiltration-based green

- 822 infrastructure in shallow groundwater environments: Challenges, approaches, and
823 progress, *Journal of Hydrology*, 2019, **579**, 124089.
- 824 44 J. Reu Junqueira, S. Serrao-Neumann and I. White, A systematic review of approaches for
825 modelling current and future impacts of extreme rainfall events using green infrastructure,
826 *Journal of Cleaner Production*, 2021, **290**, 125173.
- 827 45 W. A. Lisenbee, J. M. Hathaway, M. J. Burns and T. D. Fletcher, Modeling bioretention
828 stormwater systems: Current models and future research needs, *Environmental Modelling
829 & Software*, 2021, **144**, 105146.
- 830 46 C. E. Nika, L. Gusmaroli, M. Ghafourian, N. Atanasova, G. Buttiglieri and E. Katsou,
831 Nature-based solutions as enablers of circularity in water systems: A review on assessment
832 methodologies, tools and indicators, *Water Research*, 2020, **183**, 115988.
- 833 47 A. Palla, I. Gnecco and L. G. Lanza, Compared performance of a conceptual and a
834 mechanistic hydrologic models of a green roof, *Hydrol. Process.*, 2012, **26**, 73–84.
- 835 48 A. Palla, I. Gnecco and L. G. Lanza, Unsaturated 2D modelling of subsurface water flow
in the coarse-grained porous matrix of a green roof, *Journal of Hydrology*, 2009, **379**, 193–
204.
- 49 A. Palla, J. J. Sansalone, I. Gnecco and L. G. Lanza, Storm water infiltration in a monitored
green roof for hydrologic restoration, *Water Science and Technology*, 2011, **64**, 766–773.
- 50 S. Baek, M. Ligaray, Y. Pachepsky, J. A. Chun, K.-S. Yoon, Y. Park and K. H. Cho,
Assessment of a green roof practice using the coupled SWMM and HYDRUS models,
Journal of Environmental Management, 2020, **261**, 109920.
- 51 K. Förster, D. Westerholt, P. Kraft and G. Lösken, Unprecedented Retention Capabilities
of Extensive Green Roofs—New Design Approaches and an Open-Source Model, *Front.
Water*, 2021, **3**, 689679.
- 52 Zhangjie Peng, Colin Smith, and Virginia Stovin, The importance of unsaturated hydraulic
conductivity measurements for green roof detention modelling, *Journal of Hydrology*,
2020, **590**, 125273.
- 53 N. She and J. Pang, Physically based green roof model, *J. Hydrol. Eng.*, 2010, **15**, 458–
464.
- 54 L. A. Rossman and W. C. Huber, *Storm water management model reference manual
volume III – water quality*, US EPA Office of Research and Development, Washington,
DC:, 2016.
- 55 W. Liu, Q. Feng, R. Wang and W. Chen, Effects of initial abstraction ratios in SCS-CN
method on runoff prediction of green roofs in a semi-arid region, *Urban Forestry & Urban
Greening*, 2021, **65**, 127331.
- 56 E. M. H. Abdalla, V. Pons, V. Stovin, S. De-Ville, E. Fassman-Beck, K. Alfredsen and T.
M. Muthanna, Evaluating different machine learning methods to simulate runoff from
extensive green roofs, *Hydrol. Earth Syst. Sci.*, 2021, **25**, 5917–5935.
- 57 C. N. Nguyen, M. A. U. R. Tariq, D. Browne and N. Muttill, Performance evaluation of
large-scale green roofs based on qualitative and quantitative runoff modeling using
MUSICX, *Water*, 2023, **15**, 549.
- 58 I. Broekhuizen, S. Sandoval, H. Gao, F. Mendez-Rios, G. Leonhardt, J.-L. Bertrand-
Krajewski and M. Viklander, Performance comparison of green roof hydrological models
for full-scale field sites, *Journal of Hydrology X*, 2021, **12**, 100093.
- 59 K. Pettersson, D. Maggiolo, S. Sasic, P. Johansson and A. Sasic-Kalagasidis, On the impact
of porous media microstructure on rainfall infiltration of thin homogeneous green roof
growth substrates, *Journal of Hydrology*, 2020, **582**, 124286.
- 60 C. T. Chai, F. J. Putuhena and O. S. Selaman, A modelling study of the event-based
retention performance of green roof under the hot-humid tropical climate in Kuching,
Water Science and Technology, 2017, **76**, 2988–2999.
- 61 M. Hellies, R. Deidda and F. Viola, Retention performances of green roofs worldwide at
different time scales, *Land Degrad Dev*, 2018, **29**, 1940–1952.
- 62 P.-A. Versini, A. Gires, I. Tchinguirinskaia and D. Schertzer, Toward an operational tool
to simulate green roof hydrological impact at the basin scale: a new version of the

- 836 distributed rainfall–runoff model Multi-Hydro, *Water Science and Technology*, 2016, **74**,
837 1845–1854.
- 838 63 L. Locatelli, O. Mark, P. S. Mikkelsen, K. Arnbjerg-Nielsen, M. Bergen Jensen and P. J.
839 Binning, Modelling of green roof hydrological performance for urban drainage
840 applications, *Journal of Hydrology*, 2014, **519**, 3237–3248.
- 841 64 M. H. N. Yio, V. Stovin, J. Werdin and G. Vesuviano, Experimental analysis of green roof
842 substrate detention characteristics, *Water Science and Technology*, 2013, **68**, 1477–1486.
- 843 65 G. Vesuviano, F. Sonnenwald and V. Stovin, A two-stage storage routing model for green
844 roof runoff detention, *Water Science and Technology*, 2014, **69**, 1191–1197.
- 845 66 H. Kasmin, V. R. Stovin and E. A. Hathway, Towards a generic rainfall-runoff model for
846 green roofs, *Water Science and Technology*, 2010, **62**, 898–905.
- 847 67 L. A. Rossman, *Storm water management model user’s manual version 5.1*, US EPA Office
848 of Research and Development, Washington, DC, 2015.
- 849 68 K. Alfredo, F. Montalto and A. Goldstein, Observed and modeled performances of
850 prototype green roof test plots subjected to simulated low- and high-intensity precipitations
851 in a laboratory experiment, *J. Hydrol. Eng.*, 2010, **15**, 444–457.
- 852 69 D. Masseroni and A. Cislighi, Green roof benefits for reducing flood risk at the catchment
853 scale, *Environ Earth Sci*, 2016, **75**, 579.
- 854 70 V. Hamouz, P. Møller-Pedersen and T. M. Muthanna, Modelling runoff reduction through
855 implementation of green and grey roofs in urban catchments using PCSWMM, *Urban
856 Water Journal*, 2020, **17**, 813–826.
- 857 71 A. Palla and I. Gnecco, A continuous simulation approach to quantify the climate condition
858 effect on the hydrologic performance of green roofs, *Urban Water Journal*, 2020, **17**, 609–
859 618.
- 860 72 W. Heber Green and G. A. Ampt, Studies on soil physics, *The Journal of Agricultural
861 Science*, 1911, **4**, 1–24.
- 862 73 David Rassam, Jirka Šimůnek, Dirk Mallants, and Martinus Th. van Genuchten, *The
863 HYDRUS-1D software package for simulating the one-dimensional movement of water,
864 heat, and multiple solutes in variably-saturated media: tutorial, version 1.00*, CSIRO Land
865 and Water, Australia, 2018.
- 866 74 M. Th. Genuchten and P. J. Wierenga, Mass transfer studies in sorbing porous media I.
867 Analytical solutions, *Soil Sci. Soc. Am. j.*, 1976, **40**, 473–480.
- 868 75 G. Pęczkowski, T. Kowalczyk, K. Szawernoga, W. Orzepowski, R. Żmuda and R.
869 Pokładek, Hydrological performance and runoff Water quality of experimental green roofs,
870 *Water*, 2018, **10**, 1185.
- 871 76 E. Burszta-Adamiak and M. Mrowiec, Modelling of green roofs’ hydrologic performance
872 using EPA’s SWMM, *Water Science and Technology*, 2013, **68**, 36–42.
- 873 77 M. Mobilia and A. Longobardi, Impact of rainfall properties on the performance of
874 hydrological models for green roofs simulation, *Water Science and Technology*, 2020, **81**,
875 1375–1387.
- 876 78 S. Jeffers, B. Garner, Derek Hidalgo, D. Hidalgo, Dionisi Daoularis, and Oscar
877 Warmerdam, Insights into green roof modeling using SWMM LID controls for detention-
878 based designs, *JWMM*, , DOI:10.14796/JWMM.C484.
- 879 79 S. S. Cipolla, M. Maglionico and I. Stojkov, A long-term hydrological modelling of an
880 extensive green roof by means of SWMM, *Ecological Engineering*, 2016, **95**, 876–887.
- 881 80 A. Ebrahimian, B. Wadzuk and R. Traver, Evapotranspiration in green stormwater
882 infrastructure systems, *Science of The Total Environment*, 2019, **688**, 797–810.
- 883 81 G. H. Hargreaves and Z. A. Samani, Reference crop evapotranspiration from temperature,
884 *Applied Engineering in Agriculture*, 1985, **1**, 96–99.
- 885 82 R. G. Allen, L. S. Pereira, D. Raes and M. Smith, Crop evapotranspiration-Guidelines for
886 computing crop water requirements-FAO Irrigation and drainage paper 56, *Fao, Rome*,
887 1998, **300**, D05109.
- 888 83 G. H. Hargreaves and R. G. Allen, History and evaluation of hargreaves evapotranspiration
889 equation, *J. Irrig. Drain Eng.*, 2003, **129**, 53–63.

- 890 84 R. N. Hilten, T. M. Lawrence and E. W. Tollner, Modeling stormwater runoff from green
891 roofs with HYDRUS-1D, *Journal of Hydrology*, 2008, **358**, 288–293.
- 892 85 S. Huang, A. Garg, G. Mei, D. Huang, R. B. Chandra and S. G. Sadasiv, Experimental
893 study on the hydrological performance of green roofs in the application of novel biochar,
894 *Hydrological Processes*, 2020, **34**, 4512–4525.
- 895 86 N. Abualfaraj, J. Cataldo, Y. Elborolusy, D. Fagan, S. Woerdeman, T. Carson and F.
896 Montalto, Monitoring and modeling the long-term rainfall-runoff response of the Jacob K.
897 Javits Center green roof, *Water*, 2018, **10**, 1494.
- 898 87 T. Carson, M. Keeley, D. E. Marasco, W. McGillis and P. Culligan, Assessing methods for
899 predicting green roof rainfall capture: A comparison between full-scale observations and
900 four hydrologic models, *Urban Water Journal*, 2015, **14**, 589–603.
- 901 88 S. Huang, D. Huang, A. Garg, M. Jiang, G. Mei and S. Pekkat, Stormwater management
902 of biochar-amended green roofs: peak flow and hydraulic parameters using combined
903 experimental and numerical investigation, *Biomass Conv. Bioref.*, DOI:10.1007/s13399-
904 020-01109-x.
- 905 89 J. Wang, A. Garg, S. Huang, Z. Wu, T. Wang and G. Mei, An experimental and numerical
906 investigation of the mechanism of improving the rainwater retention of green roofs with
907 layered soil, *Environ Sci Pollut Res*, 2022, **29**, 10482–10494.
- 908 90 Filip Stanić, Yu-Jun Cui, Pierre Delage, Emmanuel De Laure, Pierre-Antoine Versini,
909 Daniel Schertzer, and Ioulia Tchiguirinskaia, A Device for the Simultaneous
910 Determination of the Water Retention Properties and the Hydraulic Conductivity Function
911 of an Unsaturated Coarse Material; Application to a Green-Roof Volcanic Substrate,
912 *Geotechnical Testing Journal*, 2019, **43**, 547–564.
- 913 91 J. Hill, B. Sleep, J. Drake and M. Fryer, The effect of intraparticle porosity and interparticle
914 voids on the hydraulic properties of soilless media, *Vadose zone j.*, 2019, **18**, 1–13.
- 915 92 R. Iffland, K. Förster, D. Westerholt, M. H. Pesci and G. Lösken, Robust vegetation
916 parameterization for green roofs in the EPA stormwater management model (SWMM),
917 *Hydrology*, 2021, **8**, 12.
- 918 93 V. Hamouz and T. M. Muthanna, Hydrological modelling of green and grey roofs in cold
919 climate with the SWMM model, *Journal of Environmental Management*, 2019, **249**,
920 109350.
- 921 94 Z. Peng and V. Stovin, Independent Validation of the SWMM Green Roof Module, *J.*
922 *Hydrol. Eng.*, 2017, **22**, 04017037.
- 923 95 G. Krebs, K. Kuoppamäki, T. Kokkonen and H. Koivusalo, Simulation of green roof test
924 bed runoff: Simulation of Green Roof Test Bed Runoff, *Hydrol. Process.*, 2016, **30**, 250–
925 262.
- 926 96 J. Leimgruber, G. Krebs, D. Camhy and D. Muschalla, Sensitivity of model-based water
927 balance to low impact development parameters, *Water*, 2018, **10**, 1838.
- 928 97 Z. Peng, C. Smith and V. Stovin, Internal fluctuations in green roof substrate moisture
929 content during storm events: Monitored data and model simulations, *Journal of Hydrology*,
930 2019, **573**, 872–884.
- 931 98 R. H. McCuen, Z. Knight and A. G. Cutter, Evaluation of the Nash–Sutcliffe efficiency
932 index, *J. Hydrol. Eng.*, 2006, **11**, 597–602.
- 933 99 B. Barnhart, P. Pettus, J. Halama, R. McKane, P. Mayer, K. Djang, A. Brookes and L. M.
934 Moskal, Modeling the hydrologic effects of watershed-scale green roof implementation in
935 the Pacific Northwest, United States, *Journal of Environmental Management*, 2021, **277**,
936 111418.
- 937 100 A. S. Basu, F. Pilla, S. Sannigrahi, R. Gengembre, A. Guiland and B. Basu, Theoretical
938 framework to assess green roof performance in mitigating urban flooding as a potential
939 nature-based solution, *Sustainability*, 2021, **13**, 13231.
- 940 101 A. G. Limos, K. J. B. Mallari, J. Baek, H. Kim, S. Hong and J. Yoon, Assessing the
941 significance of evapotranspiration in green roof modeling by SWMM, *Journal of*
942 *Hydroinformatics*, 2018, **20**, 588–596.
- 943 102 R. Hakimdavar, P. J. Culligan, M. Finazzi, S. Barontini and R. Ranzi, Scale dynamics of

- 944 extensive green roofs: Quantifying the effect of drainage area and rainfall characteristics
945 on observed and modeled green roof hydrologic performance, *Ecological Engineering*,
946 2014, **73**, 494–508.
- 947 103 A. W. Sims, C. E. Robinson, C. C. Smart and D. M. O’Carroll, Mechanisms controlling
948 green roof peak flow rate attenuation, *Journal of Hydrology*, 2019, **577**, 123972.
- 949 104 V. Stovin, S. Poë and C. Berretta, A modelling study of long term green roof retention
950 performance, *Journal of Environmental Management*, 2013, **131**, 206–215.
- 951 105 S. Poë, V. Stovin and C. Berretta, Parameters influencing the regeneration of a green roof’s
952 retention capacity via evapotranspiration, *Journal of Hydrology*, 2015, **523**, 356–367.
- 953 106 E. Cristiano, S. Urru, S. Farris, D. Ruggiu, R. Deidda and F. Viola, Analysis of potential
954 benefits on flood mitigation of a CAM green roof in Mediterranean urban areas, *Building
955 and Environment*, 2020, **183**, 107179.
- 956 107 C. Szota, C. Farrell, N. S. G. Williams, S. K. Arndt and T. D. Fletcher, Drought-avoiding
957 plants with low water use can achieve high rainfall retention without jeopardising survival
958 on green roofs, *Science of The Total Environment*, 2017, **603–604**, 340–351.
- 959 108 J. Herrera, G. Flamant, J. Gironás, S. Vera, C. Bonilla, W. Bustamante and F. Suárez, Using
960 a Hydrological Model to Simulate the Performance and Estimate the Runoff Coefficient of
961 Green Roofs in Semiarid Climates, *Water*, 2018, **10**, 198.
- 962 109 G. Brunetti, I.-A. Papagrorgiou and C. Stumpp, Disentangling model complexity in green
963 roof hydrological analysis: A Bayesian perspective, *Water Research*, 2020, **182**, 115973.
- 964 110 L. Yao, Z. Wu, Y. Wang, S. Sun, W. Wei and Y. Xu, Does the spatial location of green
965 roofs affects runoff mitigation in small urbanized catchments?, *Journal of Environmental
966 Management*, 2020, **268**, 110707.
- 967 111 S. De-Ville, M. Menon, X. Jia, G. Reed and V. Stovin, The impact of green roof ageing on
968 substrate characteristics and hydrological performance, *Journal of Hydrology*, 2017, **547**,
969 332–344.